Out-of-equilibrium nanosystems

Pierre Gaspard

Center for Nonlinear Phenomena and Complex Systems, Université Libre de Bruxelles, Campus Plaine, Code Postal 231, B-1050 Brussels, Belgium

Recent advances in the nonequilibrium statistical mechanics and thermodynamics of out-of-equilibrium nanosystems are reviewed. Nanosystems can be out of equilibrium either during their relaxation toward an equilibrium state, or when maintained in a nonequilibrium steady state imposed by external reservoirs of heat or particles at different temperatures or chemical potentials. Examples are sliding carbon nanotubes, evaporating nanoclusters, fluids in nanohydrodynamics, mesoscopic conductors, and biological molecular motors. Remarkable relations have been recently discovered in the properties of their fluctuating paths or histories during some time interval. These advances give a new understanding to the second law of thermodynamics in terms of the time asymmetry in the dynamical randomness of these paths or histories.

§1. Introduction

Natural phenomena are striking us every day by the time asymmetry of their evolution. Various examples of this time asymmetry exist in physics, chemistry, biology, and the other natural sciences. This asymmetry manifests itself in the dissipation of energy due to friction, viscosity, heat conductivity, or electric resistivity, as well as in diffusion and chemical reactions. The second law of thermodynamics formulates the time asymmetry in terms of the increase of the entropy. The aforementioned irreversible processes are fundamental for biological systems since they are maintained out of equilibrium by their metabolic activity.

These nonequilibrium phenomena exist from the macroscopic level down to the nanoscale, as shown by recent work in nanosciences. Nanosystems are studied not only for their structure but also for their functional properties. Examples are the electronic and mechanical properties of single molecules, the kinetics of molecular motors, or the physics and chemistry of nanoclusters. Many examples of nanosystems are found in biological systems, which display structures on all scales down to the nanometer. The nanoscale is important because it is the scale just above the size of the atoms, which marks the beginning of the complexification of matter into structures of larger and larger spatial sizes and correlated motions on longer and longer time scales. The nanoscale is thus the scale from where collective behaviors emerge in the assemblies of atoms and molecules. However, because of their small size, nanosystems and their properties such as the currents are affected by molecular fluctuations. These fluctuations are described by nonequilibrium statistical mechanics, which therefore find today important applications in nanosciences. Traditionally, statistical mechanics is concerned with macroscopic properties and its application to nanosystems is a challenge which is met thanks to recent advances coming from dynamical systems theory. The purpose of dynamical systems theory is to analyze the

Progress of Theoretical Physics Supplement **165** (2006) 33-56

trajectories of systems having a finite number of degrees of freedom and to describe their statistical properties in terms of invariant probability measures. This theory has been developed during the last decades and new concepts have been introduced to understand, in particular, how deterministic systems ruled by ordinary differential equations such as Newton's equation can generate random time evolutions, the so-called chaotic behaviors. These new concepts have been used to revisit statistical mechanics and to gain insights into the properties of the fluctuations in nonequilibrium systems. New relationships have been derived such as the escape-rate and chaos-transport formulae,[1)–8)] the fluctuation theorem,[9)–20)] and the nonequilibrium work theorem,[21)] which are all based on the description of nonequilibrium systems in terms of paths or histories during given time intervals. Different quantities can be associated with a path or history such as the dynamical instability characterized by finite-time Lyapunov exponents, the dynamical randomness and the lack of detailed balance defined in terms of the invariant probability measure of a path or history, the work dissipated or performed by the system, the currents crossing the system, the numbers of molecules produced by a reaction, or the rotation angle of a molecular motor. These quantities can take a different value for each path or history because of the fundamental molecular fluctuations. Their statistical distributions present remarkable properties, which have been formulated in terms of these new relationships.

These new methods from nonequilibrium statistical mechanics can be applied to understand the properties of out-of-equilibrium nanosystems. We can here distinguish four classes of out-of-equilibrium nanosystems: (1) those presenting a relaxation toward a state of equilibrium; (2) the systems with a nonequilibrium transient behavior until a first passage beyond some threshold; (3) the systems maintained in a nonequilibrium steady state by external reservoirs; (4) the systems driven by time-dependent external forces. Each class has its own methods of description in nonequilibrium statistical mechanics. In the first class, we present the case of friction in the sliding motion of two carbon nanotubes. The second class is covered by the escape-rate theory, which has applications in micro- and nanohydrodynamics. In the third class, we shall describe biological nanomotors and electronic transport in mesoscopic conductors, to which the fluctuation theorem can be applied. The fourth class contains single molecules manipulated by optical tweezers or atomic force nanoscopes and to which Jarzynski's nonequilibrium work theorem and Crooks fluctuation theorem apply.[22),23)]

As in all out-of-equilibrium systems, entropy is produced in a nanosystem maintained in a nonequilibrium steady state. However, nanosystems are affected by fluctuations and we may wonder how entropy production can be measured at the nanoscale. Very recently, a new relationship have been derived showing that the origin of entropy production can be attributed to a time asymmetry in the dynamical randomness of nonequilibrium steady states.[24),25)] Dynamical randomness is the property that the paths or histories of a fluctuating nanosystem do not repeat themselves and present stochastic time evolutions. The paths or histories of such stochastic processes can be depicted in space-time plots, representing the random time evolution of their state. It is known since the work of Boltzmann that the

thermodynamic entropy is a measure of the disorder of the state of the system at a given time. In contrast, the dynamical randomness can be characterized by the concept of entropy per unit time, which is a measure of disorder along the time axis instead of the space axes.[26)–28)] Under nonequilibrium conditions, a time asymmetry appears in the dynamical randomness measured either forward or backward in time with the so-called Kolmogorov-Sinai entropy per unit time[27),28)] or the newly introduced time-reversed entropy per unit time.[24),25)] The difference between both quantities is precisely the entropy production of nonequilibrium thermodynamics. This new relationship allows one to measure the entropy production from the observation of the fluctuations in nonequilibrium systems. Furthermore, this new result provides an interpretation of the second law of thermodynamics in terms of temporal ordering out of equilibrium, which has far reaching consequences in biology as will be explained below.

The plan of the paper is the following. Section 2 is devoted to the nanosystems presenting a relaxation toward a state of equilibrium from the viewpoint of dynamical systems theory. In Sec. 3, it is explained how kinetic and transport properties can be obtained in nanosystems by considering first passage problems. Nanosystems maintained in nonequilibrium steady states are described in Sec. 4. In Sec. 5, their fluctuation properties are described and fluctuation theorems are formulated for the currents and the dissipated work. Furthermore, generalizations of Onsager reciprocity relations to nonlinear response are given. The time asymmetry in the dynamical randomness of nonequilibrium nanosystems is presented in Sec. 6. Conclusions are drawn in Sec. 7.

§2. Relaxation of nanosystems toward an equilibrium state

2.1. *The statistical description of motion*

In this section, we consider isolated nanosystems and their dynamics. Examples are clusters of atoms or molecules, as well as single-walled or multi-walled nanotubes. At low temperature, these systems are ruled by Schrödinger's equation of quantum mechanics. At higher temperature, Newton's equation of classical mechanics suffices to describe their dynamics. Newton's equation is equivalent to Hamilton's equations for the positions $\{\boldsymbol{r}_a\}_{a=1}^N$ and momenta $\{\boldsymbol{p}_a\}_{a=1}^N$ of the N particles composing the system:

$$\frac{d\boldsymbol{r}_a}{dt} = +\frac{\partial H}{\partial \boldsymbol{p}_a} \qquad\qquad \frac{d\boldsymbol{p}_a}{dt} = -\frac{\partial H}{\partial \boldsymbol{r}_a} \tag{2·1}$$

with $a = 1, 2, ..., N$. The Hamiltonian function H is the energy of the system which is conserved if the system is not submitted to time-dependent external forces. The solution of Hamilton's equations is unique for given initial positions and momenta. The integration of Hamilton's equations thus results into a unique trajectory issued from the initial conditions, which is the mathematical expression of determinism. The trajectory is a curve in the phase space $\boldsymbol{\Gamma} = \{\boldsymbol{r}_a, \boldsymbol{p}_a\}_{a=1}^N$. Liouville's theorem guarantees that the phase-space volumes are preserved by Hamiltonian dynamics.

The system (2·1) of Hamilton's equations is symmetric under time reversal

$t \to -t$, $\boldsymbol{r}_a \to \boldsymbol{r}_a$, and $\boldsymbol{p}_a \to -\boldsymbol{p}_a$ if the Hamiltonian is an even function of the momenta. This means that the time-reversed trajectory $[\boldsymbol{r}_a(-t), -\boldsymbol{p}_a(-t)]$ is solution of Hamilton's equation if the trajectory $[\boldsymbol{r}_a(t), \boldsymbol{p}_a(t)]$ is. This property is called *microreversibility*. We notice that microreversibility does not mean that the trajectory itself is time-reversal symmetric. For typical systems, most of the trajectories do not have the time-reversal symmetry of the equations, i.e., the time-reversed trajectory $[\boldsymbol{r}_a(-t), -\boldsymbol{p}_a(-t)]$ is physically distinct from the trajectory $[\boldsymbol{r}_a(t), \boldsymbol{p}_a(t)]$ itself. The situation is similar to the well-known phenomenon of spontaneous breaking of symmetry that the solution of an equation may break the symmetry of the equation. In the present context, we shall refer to this phenomenon as *time asymmetry*. In this sense, the time asymmetry of some trajectories is compatible with the microreversibility of Newton's or Hamilton's equations.[29)]

Experiments on nanosystems such as atomic or molecular clusters deal with a statistical ensemble of systems, which is described by a probability distribution. This distribution is defined by a probability density, which is a function of the positions and momenta of all the particles. Since probability is conserved in the phase space, it obeys a continuity equation called Liouville's equation:

$$\partial_t\, p = -\mathrm{div}(\dot{\boldsymbol{\Gamma}} p) = \{H, p\} \equiv \hat{L} p \tag{2·2}$$

which is given in terms of the so-called Liouvillian operator. This operator is defined by the Poisson bracket of the Hamiltonian with the probability density $p(\boldsymbol{\Gamma}; t)$ according to Liouville's theorem. Liouville's equation is time-reversal symmetric as a consequence of microreversibility. As for Hamilton's equations, the solutions of Liouville's equation does not need to have this symmetry, in which case the solution is time asymmetric.

The probability density allows us to define the statistical averages of the different observables $A(\boldsymbol{\Gamma})$ of the system as

$$\langle A \rangle_t = \int A(\boldsymbol{\Gamma})\; p(\boldsymbol{\Gamma}; t)\; d\boldsymbol{\Gamma} \tag{2·3}$$

The system is said to be *mixing* if such averages tend toward a stationary value after a time long enough for the system to have forgotten its initial conditions.[30)] Mixing is possible for isolated classical systems, as well as for classical or quantum systems in contact with a thermal bath at a given temperature. In the first case, the asymptotic value of the statistical average corresponds to the microcanonical statistical ensemble if all the trajectories have the same energy. In the second case, the statistical average tends to the value corresponding to the canonical statistical ensemble. Therefore, the mixing property is useful to describe the relaxation of the system toward a statistical state corresponding to the thermodynamic equilibrium. The equilibrium state represents a statistical ensemble of copies of the system. These copies are generated for instance in beams of atomic or molecular clusters in typical experiments. Whether a system is mixing or not depends on its intrinsic dynamical properties.[30)] For instance, a fully integrable system presents quasiperiodic motion and is not mixing. Examples of mixing systems are the baker map, the Bunimovich stadium billiard, and the hard-disk Lorentz gases.

2.2. *The Pollicott-Ruelle resonances*

A remarkable result is that the decay of the statistical averages at long times can be decomposed in terms of the singularities of the spectral function

$$S(\omega) = \int_{-\infty}^{+\infty} dt\, \mathrm{e}^{i\omega t} \langle A \rangle_t \tag{2·4}$$

at complex values of the frequency ω. In the case that the singularity is a complex pole, we speak about a Pollicott-Ruelle resonance.[31),32)] Branch cuts and other singularities are possible. The statistical average can be recovered by the inverse Fourier transform of the spectral function as

$$\langle A \rangle_t = \frac{1}{2\pi} \int_{-\infty}^{+\infty} d\omega\, \mathrm{e}^{-i\omega t} S(\omega) \tag{2·5}$$

The integral over the frequency can be deformed into an integration contour at complex frequencies $z = \omega \pm i\gamma$ in order to pick up the contributions of the poles and other singularities. A decomposition valid for positive times is obtained if the analytic continuation is performed toward the complex frequencies with negative imaginary part, which defines the so-called forward semigroup. This decomposition gives a sum of exponential decays $\exp(-\gamma t - i\omega t)$ corresponding to each Pollicott-Ruelle resonances with possible power-law decays coming from the branch cuts. A similar decomposition holds at negative times for the backward semigroup. This mathematical method allows us to understand how exponential decays – which are paradigmatic of irreversible processes – can arise in Hamiltonian systems. It is the analytic continuation toward complex frequencies which is responsible for the breaking of time-reversal symmetry. The Pollicott-Ruelle resonances can be viewed as generalized eigenvalues $s = -iz = -\gamma - i\omega$ of the Liouvillian operator: $\hat{L}\Psi = s\Psi$. The invariant probability density corresponding to the equilibrium state is an eigenstate of vanishing eigenvalue $s = 0$. This eigenstate has the time-reversal symmetry. However, this symmetry is broken for the eigenstates associated with complex frequencies of nonvanishing imaginary part $\gamma \neq 0$ and corresponding to some decay. The description of the time evolution in terms of these decaying states is thus time asymmetric as a consequence of the selection of the statistical ensemble of initial conditions.

Pollicott-Ruelle resonances and their associated eigenstates have been explicitly constructed in several systems such as one-dimensional maps, the multibaker map, the hard-disk scatterers, the hard-disk and Yukawa-potential Lorentz gases.[6),33)] These resonances have also been studied in wave scattering on hard disks,[34)–37)] in quantum spin chains,[38)] and in quantum systems coupled to a thermal environment such as the spin-boson system or the diffusion of a quantum particle.[39),40)] In all these systems, the resonances control the relaxation toward the equilibrium state. They are thus associated with the irreversible processes responsible for this relaxation. In spatially extended systems sustaining the transport property of diffusion, the leading Pollicott-Ruelle resonances take the form, $s = -Dk^2 + O(k^4)$, where D is the diffusion coefficient and k is the wavenumber of the associated eigenstate. Accordingly, the value of the transport coefficients can be calculated from

the Pollicott-Ruelle resonances. An important remark is the following. If the relaxation of a system can be modeled by a Fokker-Planck equation or some other kinetic master equation of nonequilibrium statistical mechanics, their eigenvalues provide approximate values of the Pollicott-Ruelle resonances. Therefore, we can conceive the relaxation of many systems toward a statistical equilibrium state in terms of these resonances and identify in this way the transport coefficients and other irreversible properties. An application of this method is given in the next subsection.

2.3. *Friction in sliding carbon nanotubes*

We consider double-walled carbon nanotubes sliding one with respect to the other in a telescoping motion.[41),42)] The dynamics of this system is ruled by the total Hamiltonian

$$H = K^{(1)} + K^{(2)} + U_{\rm TB}^{(1)} + U_{\rm TB}^{(2)} + \sum_{a=1}^{N_1}\sum_{b=1}^{N_2} U_{\rm LJ}\left(\|\boldsymbol{r}_a^{(1)} - \boldsymbol{r}_b^{(2)}\|\right) \qquad (2\cdot6)$$

where $K^{(1)}$ and $K^{(2)}$ are respectively the kinetic energies of the inner and outer nanotubes while $U_{\rm TB}^{(1)}$ and $U_{\rm TB}^{(2)}$ are the Tersoff-Brenner potentials of both nanotubes. The positions and momenta of the carbon atoms of both nanotubes are denoted by $\{\boldsymbol{r}_a^{(i)}\}_{a=1}^{N_i}$ and $\{\boldsymbol{p}_a^{(i)}\}_{a=1}^{N_i}$ with $i=1$ (resp. $i=2$) for the inner (resp. outer) tube. The kinetic energies are given by $K^{(i)} = (1/2m)\sum_{a=1}^{N_i}(\boldsymbol{p}_a^{(i)})^2$, where $m = 12$ amu is the mass of a carbon atom. The intertube potential is modeled by a 6-12 Lennard-Jones potential $U_{\rm LJ}$.

Systems as the one of Fig. 1 containing about 1300 carbon atoms can be simulated by the molecular-dynamics method based on a velocity Verlet algorithm. The dynamics conserves energy and is time-reversal symmetric. The simulation reveals oscillations in the quasi one-dimensional relative motion of the centers of mass of each nanotube. These oscillations are damped due to the friction between the nanotubes. As a consequence, the energy in the single degree of freedom of the relative motion is transferred to the many vibrational degrees of freedom of each nanotube. Therefore, the amplitude of the oscillations of the relative motion decreases in time. The dynamics has three characteristic time scales:

1. The vibrational time scale given by the inverse of the Debye vibrational frequency of the carbon nanotubes: $t_{\rm C} \simeq 50$ fs. This time scale is also referred to as the correlation time which is the decay time of the autocorrelation function of the force between the nanotubes.
2. The period of oscillations: $t_{\rm P} \simeq 10$ ps.
3. The relaxation time: $t_{\rm R} \simeq 1000$ ps.

After the relaxation time, the system has reached a statistical equilibrium state in which the oscillations have random amplitudes (see Fig. 1). It is an important remark that each individual system continues its motion and that this motion has statistical properties described by the equilibrium probability distribution. This equilibrium probability distribution corresponds to the microcanonical ensemble of the initial energy in which the atoms have an approximate Maxwell velocity distribution at a temperature of about 338 K.

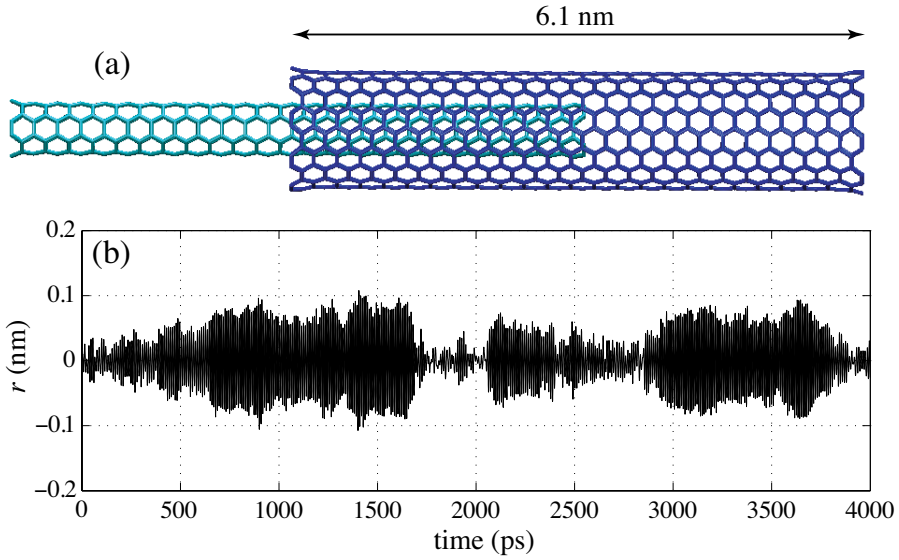

Fig. 1. (a) The double-walled armchair-armchair carbon nanotubes (4,4)@(9,9) with $N_1 = 400$ and $N_2 = 900$ carbon atoms. (b) Fluctuating oscillations of the relative position r between the centers of mass of the nanotubes in the microcanonical equilibrium state at $T \simeq 338$ K.[42)]

The observed behaviors can be modeled by an effective Langevin-type Newtonian equation

$$\mu \frac{d^2 r}{dt^2} = -\frac{dV(r)}{dr} + F_{\text{frict}} + F_{\text{fluct}}(t) \tag{2·7}$$

where r is the distance between the centers of mass and $\mu = mN_1N_2/(N_1 + N_2)$ is their relative mass. $V(r)$ is the van der Waals potential of interaction between both nanotubes which has a V-shape. Indeed, this interaction is proportional to the number of van der Waals bonds between the nanotubes and this number is proportional to the length of the overlap between the two nanotubes. The potential is well fitted by

$$V(r) = F\sqrt{r^2 + l^2} - C \simeq \begin{cases} F|r| - C & \text{for } l \ll |r| \\ \frac{k}{2} r^2 + Fl - C & \text{for } |r| \ll l \end{cases} \tag{2·8}$$

with $k = F/l$ and $l = 0.2$-0.3 nm.[42)]

Beside the conservative force of the van der Waals interaction, there is a dynamical friction force because of the energy dissipation from the one-degree-of-freedom oscillatory motion to the many degrees of freedom of vibration of the carbon atoms around their equilibrium positions in the nanotubes. For relative velocities which are not too large, the dynamic friction force is well approximated as

$$F_{\text{frict}} = -\zeta\, v + O\left(v^2\right) \qquad \text{with} \quad v = \frac{dr}{dt} \tag{2·9}$$

The friction coefficient is given by Kirkwood formula

$$\zeta \simeq \frac{1}{k_{\rm B}T}\int_0^\tau \left[\langle F_{\rm vdW}(t)\,F_{\rm vdW}(0)\rangle_{E,r} - \langle F_{\rm vdW}\rangle^2_{E,r}\right]\,dt \tag{2·10}$$

in terms of the time integral of the autocorrelation function of the van der Waals force between both nanotubes. This autocorrelation function should be integrated till a cutoff time τ where the integral reaches a plateau value. The friction coefficient (2·10) is approximately constant over an important range of values of the relative position r. This friction coefficient is responsible for the energy dissipation and the damping of the amplitudes of the oscillations. For initial amplitudes which are large with respect to the fluctuations, the effect of the Langevin force can be neglected. In this case, both the amplitudes of the oscillations and the energy $E = (\mu/2)v^2 + V(r)$ can be shown to be exponentially damped at the rate $\Gamma = 2\zeta/(3\mu)$.[42] The value of this damping rate obtained from molecular-dynamics simulation is consistent with the value of the friction coefficient given by Kirkwood formula, which validates the assumption of a dynamic friction force proportional to the relative velocity.[42]

On long times, the amplitudes of the oscillations become too small to further neglect the Langevin force. This fluctuating force is related to the one considered in Kirkwood formula $F_{\rm fluct} \simeq F_{\rm vdW} - \langle F_{\rm vdW}\rangle$. The autocorrelation of this force decays over the correlation time scale, $t_{\rm C} \simeq 50$ fs, which is very small with respect to both the period of oscillations and the relaxation time. Accordingly, the fluctuating force can be supposed to be a Gaussian white noise such that

$$\langle F_{\rm fluct}(t)\rangle = 0 \qquad\qquad \langle F_{\rm fluct}(t)F_{\rm fluct}(t')\rangle = 2\,\zeta\,k_{\rm B}\,T\,\delta(t-t') \tag{2·11}$$

for $|t-t'| \gg t_{\rm C}$. The time evolution of the probability density $p(r,v;t)$ that the system has the relative position r and velocity v is thus ruled by the Fokker-Planck equation

$$\frac{\partial p}{\partial t} = -v\,\frac{\partial p}{\partial r} + \frac{\partial}{\partial v}\left[\frac{1}{\mu}\left(\frac{dV}{dr} + \zeta v\right)p\right] + \frac{\zeta k_{\rm B}T}{\mu^2}\frac{\partial^2 p}{\partial v^2} \tag{2·12}$$

This equation describes the relaxation of the nanosystem toward the equilibrium state

$$p_{\rm eq}(r,v) = \frac{1}{Z}\,\exp\left\{-\frac{1}{k_{\rm B}T}\left[\frac{\mu}{2}v^2 + V(r)\right]\right\} \tag{2·13}$$

which corresponds to the eigenvalue $s = 0$. We notice that, in this equilibrium state, the relative position undergoes a very small fluctuating motion of amplitude $\sqrt{\langle r^2\rangle_{\rm eq}} = \sqrt{lk_{\rm B}T/F} \simeq 0.04$ nm (see Fig. 1). This motion takes place in the region where the intertube potential is nearly harmonic. Supposing that $dV/dr = -kr$, the eigenvalues of the Fokker-Planck equation are given by

$$s_{mn} = m\,s_+ + n\,s_- \qquad \text{with} \quad s_\pm = -\frac{\zeta}{2\mu} \pm i\sqrt{\frac{k}{\mu} - \left(\frac{\zeta}{2\mu}\right)^2} \tag{2·14}$$

and $m, n = 0, 1, 2, 3, ...$ This oscillator is underdamped because the relaxation time is longer than the period. The system would be overdamped if the friction coefficient was larger, for instance, in a liquid environment. The eigenvalues (2·14) give

approximations for the Pollicott-Ruelle resonances of the system. The statistical averages as well as the correlation functions of the system thus decay as combinations of $\exp(s_{mn}t)$ toward their equilibrium value.

It is remarkable that such a nanosystem containing about a thousand atoms can already present a typical irreversible behavior such as the relaxation toward an equilibrium state under the effect of friction. In other circumstances, energy is injected into the system to compensate for its dissipation due to friction and to sustain the motion, as in nanomotors which uses multiple-walled carbon nanotubes as shaft and electrostatic force for driving.[44] In this case, it is the rotational friction which dissipates the energy injected by the external driving.

We notice that the damping of collective oscillations also exist in other nanosystems such as atomic and molecular clusters and can be treated similarly.

§3. First-passage problems in nanosystems

3.1. *Examples*

Instead of following the trajectory of a system on time scales longer than the relaxation time, we can wait till the trajectory crosses for the first time some threshold in the phase space and record this escape time. The experiment can be repeated many times from statistically distributed initial conditions and the statistics of the escape times will characterize the physical property associated with the threshold. Such a gedanken experiment is called a first-passage problem and it was considered in particular by Kramers for the passage of a Brownian particle above a barrier. The number of trajectories which have not crossed the threshold by the time t, divided by the initial number of trajectories, defines the probability for a trajectory to remain below the threshold till the time t. This survival probability can in principle be calculated by solving Liouville's equation with absorbing boundary conditions on the phase-space hypersurface corresponding to the threshold. Typically, the survival probability decays exponentially as

$$P(t) = \frac{\mathcal{N}(t)}{\mathcal{N}(0)} \sim \exp(-\gamma t) \tag{3·1}$$

which defines the escape rate γ.[6] In this case, the escape rate is the leading Pollicott-Ruelle resonance of Liouville's equation: $\hat{L}\,\Psi = -\gamma\,\Psi$. To be specific, let us consider a few examples (see Fig. 2).

3.1.1. Effusion

The process of effusion is the escape of particles from a container of volume V filled with a rarefied gas (see Fig. 2a).[45] The particles escape through a hole of area A. The gas is rarefied under the condition that the mean free path of the particles in the gas is larger than the diameter of the hole. Under this condition, the particles escape independently of each other and the escape rate can be calculated by simple kinetic considerations. The flux of particles through the hole is given by

$$\phi = \frac{\overline{v}}{4}\, n\, A = k\, N \qquad \text{with} \quad k = \frac{\overline{v}\, A}{4\, V} \tag{3·2}$$

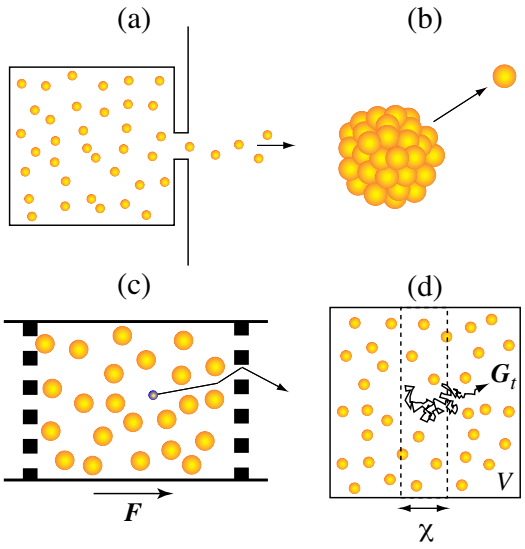

Fig. 2. First-passage problems in nanosystems: (a) Effusion of a rarefied gas through a hole. (b) Evaporation of a hot nanocluster. (c) Diffusive motion and escape of a charged particle from a fluid of neutral particles through semi-permeable walls. (d) Diffusive motion of the Helfand moment associated with viscosity or heat conductivity and its escape from the region delimited by the dashed lines for a fluid in a container of volume V.

where $\overline{v} = \sqrt{8k_{\rm B}T/(\pi m)}$ is the mean speed of the particles, $n = N/V$ is the density of particles in the container, and k is the effusion constant. The process is stochastic and ruled by the master equation

$$\frac{dP(N;t)}{dt} = -k\,N\,P(N;t) + k\,(N+1)\,P(N+1;t) \tag{3·3}$$

where $P(N;t)$ denotes the probability that N particles are inside the container. The mean number of particles $\langle N\rangle = \sum_{N=0}^{\infty} NP(N;t)$ obeys the equation

$$\frac{d\langle N\rangle}{dt} = -k\,\langle N\rangle \tag{3·4}$$

at the rate given by effusion constant. This is the rate of escape of particles from the container. However, the process involves many particles so that the phase space of the microscopic dynamics is of dimension equal to $6N$ before the escape of a particle. The threshold should therefore correspond to the transition $N \to N-1$ in the multiparticle phase space. The state with $N-1$ particles is thus an absorbing state for the master equation (3·3) and its eigenvalues are given by

$$s = -kN,\ -k(N+1),\ -k(N+2),\ ... \tag{3·5}$$

The escape rate of the trajectories is given by the leading of these eigenvalues as $\gamma = kN$. This example shows that an important difference exists between the escape rate of particles which is given by the effusion constant k and the escape rate of trajectories kN which is proportional to the number N of particles. For an ideal

gas, the particles are independent of each other during their whole time evolution so that the problem decomposes into the dynamics of a single particle in the container. The escape is exponential if the walls of the container are defocusing, otherwise power-law decays are possible.

3.1.2. Evaporation of a nanocluster

Another example concerns the evaporation of a nanocluster containing N atoms or molecules at high temperature (see Fig. 2b). The transition $N \to N-1$ corresponds to the dissociation of one particle from the cluster of size N. This process can be simulated by molecular dynamics based on Hamilton's equations (2·1). The dissociation corresponds to the separation of the position of any particle from the center of mass of the $N-1$ other particles by a distance larger than the radius of the cluster, which is a hypersurface in the phase space of the N-particle system. The survival probability decays exponentially as Eq. (3·1) with an escape rate γ giving the dissociation rate. The problem is similar as for unimolecular reactions in chemical kinetics. For a statistical ensemble of clusters at fixed temperature T, the dissociation rate can be evaluated by Arrhenius' law

$$\gamma \simeq \nu \; N^{2/3} \; \exp(-D_N/k_{\rm B}T) \tag{3·6}$$

where ν is an attempt frequency for overcoming the barrier of the dissociation energy D_N.[46] The dissociation rate is proportional to the area, hence the factor $N^{2/3}$. The escape rate γ gives the leading Pollicott-Ruelle resonance $s = -\gamma$ of the Liouvillian dynamics.

3.1.3. Diffusion and mobility

First-passage problems can also be set up for transport properties, in particular, for the diffusion of a charged particle in a medium and its mobility under the effect of a force field $\boldsymbol{F}$. We can suppose that the charged particle moves in a fluid of neutral particles confined between two semi-permeable walls allowing the passage of the charged particle but not the neutral ones (see Fig. 2c). This system can be simulated by a Hamiltonian dynamics in order to obtain the statistics of the escape times of the charged particle. On large spatial scales and long times, the motion of the charged particle is described by the Fokker-Planck equation:

$$\partial_t \, p = \boldsymbol{\nabla} \cdot (D \, \boldsymbol{\nabla} p - \mu \, \boldsymbol{F} \, p) \tag{3·7}$$

with the diffusion coefficient D and the mobility μ. In a multiparticle system at temperature T, these coefficients are linked by Einstein's relation $D = \mu k_{\rm B} T$. The first-passage problem is formulated by taking absorbing boundary conditions such that $p(x = 0, y, z; t) = p(x = L, y, z; t) = 0$ for all times t if the force is oriented in the x-direction perpendicular to the semi-permeable walls separated by the distance L. The eigenvalues of the Fokker-Planck equation are given by

$$s = -\frac{\mu^2 F^2}{4D} - D \, k^2 \tag{3·8}$$

where the wavenumber takes the values $k = (\pi j/L)^2$ with $j = 1, 2, 3, ...$[6),47)] The leading eigenvalue for $j = 1$ is the escape rate

$$\gamma = \frac{\mu^2 F^2}{4D} + D\left(\frac{\pi}{L}\right)^2 \tag{3·9}$$

Therefore, it is possible to determine both the diffusion coefficient and the mobility by carrying out an experiment measuring the statistics of the escape times in the limits $F \to 0$ and $L \to \infty$.

3.1.4. Shear viscosity and heat conductivity

The same method can be applied to collective transport properties such as shear viscosity and heat conductivity in small systems of particles as encountered in nanohydrodynamics. The key quantities are the so-called Helfand moments which are associated with each transport property:

$$\text{shear viscosity:} \qquad G^{(\eta)} = \frac{1}{\sqrt{V k_{\rm B} T}} \sum_{a=1}^{N} x_a \, p_{ay} \tag{3·10}$$

$$\text{heat conductivity:} \qquad G^{(\kappa)} = \frac{1}{\sqrt{V k_{\rm B} T^2}} \sum_{a=1}^{N} x_a \, (E_a - \langle E_a \rangle) \tag{3·11}$$

where the energy of the particle a is defined by $E_a = \frac{\boldsymbol{p}_a^2}{2m} + \frac{1}{2}\sum_{b(\neq a)} U(r_{ab})$.[3),4)] The Helfand moments represent the centroid of the momenta or energies of the particles in the fluid.[48)] The time derivative of a Helfand moment gives the microscopic current entering the Green-Kubo formula.[49),50)] Each transport coefficient is obtained from its corresponding Helfand moment by Einstein's formula

$$\alpha = \lim_{t\to\infty} \frac{1}{2t} \langle \Big[\Delta G^{(\alpha)}(t) - \Delta G^{(\alpha)}(0) \Big]^2 \rangle \tag{3·12}$$

with $\Delta G^{(\alpha)} = G^{(\alpha)} - \langle G^{(\alpha)} \rangle$. This shows that the Helfand moment is performing a random walk in the space where it is defined according to the Fokker-Planck equation

$$\partial_t \, p = \alpha \, \partial_g^2 \, p \tag{3·13}$$

We can thus consider a problem of first passage of the Helfand moment at some thresholds where $g = \Delta G^{(\alpha)}(t) = \pm\chi/2$ (see Fig. 2d). This corresponds to the absorbing boundary conditions $p(g = \pm\chi/2; t) = 0$ for the Fokker-Planck equation (3·13).[3)] These boundaries in the space of the Helfand moment correspond to hypersurfaces in the phase space of the Hamiltonian system. The Hamiltonian trajectories can escape from the domain delimited by these hypersurfaces and an escape rate γ can be associated with this process:

$$s = -\gamma = -\alpha \left(\frac{\pi}{\chi}\right)^2 \tag{3·14}$$

This escape rate is here also the leading Pollicott-Ruelle resonance $s = -\gamma$ of the corresponding Liouvillian operator. The transport coefficient α which is either the

shear viscosity or the heat conductivity can be obtained from the escape rate if χ is large enough. The properties of viscosity or heat conductivity can be ill defined if the fluid is too small but the escape rate can still be well defined, which shows that the escape-rate theory is appropriate for systems with a finite number of particles. Furthermore, it is possible to obtain good values of the viscosity coefficient in small systems with periodic boundary conditions by spatial extension of the Helfand moment.[51),52)]

3.2. *Escape-rate formula*

The escape rate can be related to the underlying microscopic Hamiltonian dynamics by the following reasoning.[1)–4)] We consider the partition of the phase space into cells C_ω which are disjoint and cover the $6N$-dimensional phase space. Each trajectory successively visits different cells during its time evolution. The cells visited at the successive times 0, Δt, $2\Delta t$,... form a sequence labeled by $\omega_0\omega_1\omega_2\cdots$, which defines the path or history associated with the trajectory. We consider the set of trapped trajectories which never escape from the phase-space domain delimited by the threshold. This set can be approximated by the trajectories which have not yet escaped after some long but finite time. The volumes of the $3N$-dimensional position space tend to increase in time by stretching factors $\Lambda(\omega_0\omega_1\omega_2\cdots\omega_{n-1})$ which may differ among the different trajectories. If the system is dynamically unstable, these stretching factors increase exponentially at rates equal to the sum of positive Lyapunov exponents:

$$\Lambda(\omega_0\omega_1\omega_2\cdots\omega_{n-1}) \sim \exp\left(\sum_{\lambda_i>0}\lambda_i t\right) \tag{3·15}$$

The sum of the inverses of these stretching factors is proportional to the phase-space region which has not yet escaped by the time $t = n\Delta t$ so that the escape rate is given by

$$\sum_{\omega_0\omega_1\omega_2\cdots\omega_{n-1}} \Lambda(\omega_0\omega_1\omega_2\cdots\omega_{n-1})^{-1} \sim \exp(-\gamma t) \tag{3·16}$$

On the other hand, the probability measure can be constructed on the set of trapped trajectories by

$$\mu(\omega_0\omega_1\omega_2\cdots\omega_{n-1}) = \frac{\Lambda(\omega_0\omega_1\omega_2\cdots\omega_{n-1})^{-1}}{\sum_{\omega_0\omega_1\omega_2\cdots\omega_{n-1}}\Lambda(\omega_0\omega_1\omega_2\cdots\omega_{n-1})^{-1}} \tag{3·17}$$

in the long-time limit $n \to \infty$. This probability measure is normalized to unity. The dynamical randomness on the set of trapped trajectories can be characterized by the decay rate of these path probabilities

$$\mu(\omega_0\omega_1\omega_2\cdots\omega_{n-1}) \sim \exp(-ht) \tag{3·18}$$

which defines the so-called entropy per unit time h. The entropy per unit time tends to the Kolmogorov-Sinai entropy per unit time for cells of arbitrarily small

diameters. The ratio of the path probability over the inverse of the corresponding stretching factor increases exponentially at the escape rate

$$\frac{\mu(\omega_0\omega_1\omega_2\cdots\omega_{n-1})}{\Lambda(\omega_0\omega_1\omega_2\cdots\omega_{n-1})^{-1}} \sim \exp(\gamma t) \tag{3·19}$$

Taking the logarithm of both sides and the limit of an arbitrarily fine partition, we obtain the escape rate formula

$$\gamma = \sum_{\lambda_i>0} \lambda_i - h_{\rm KS} \tag{3·20}$$

which relates the characteristic quantities of the microscopic dynamics to irreversible properties such as the transport coefficients and the effusion or evaporation rates. The escape-rate formula is a dynamical large-deviation relationship concerned by the properties of instability and randomness of the paths or histories. It has been used to calculate diffusion and viscosity coefficients.[2),51),52)] Further similar relationships such as the fluctuation theorem will be given below for other path properties.

§4. Nanosystems maintained out of equilibrium

4.1. *Description of nanosystems in nonequilibrium steady states*

A nanosystem can be maintained out of equilibrium if it is in contact with several reservoirs of heat or particles at different temperatures or chemical potentials. This is the case for a conducting molecule in an electric circuit or a molecular motor in a difference of Gibbs free energy between the chemical reactants and products. Such systems are open so that a Hamiltonian description would *a priori* involve an infinite number of particles. These infinite systems admit a probabilistic description based on an invariant probability measure associated with the nonequilibrium steady state which establishes itself between the reservoirs after long enough times. The particles coming from the reservoirs enter into the system with positions and momenta determined from the dynamics external to the system. A reduced description can be adopted if the incoming fluxes of energy or particles are supposed to be ruled by stochastic processes. In many applications, the state of the system between the reservoirs follows a stochastic path or history obeying a Markovian master equation

$$\frac{d}{dt}P_t(\sigma) = \sum_{\rho,\sigma'(\neq\sigma)} \left[P_t(\sigma')\,W_\rho(\sigma'|\sigma) - P_t(\sigma)\,W_{-\rho}(\sigma|\sigma')\right] \tag{4·1}$$

where $P_t(\sigma)$ is the probability to find the system in the state σ by the time t.[53)–56)] The states can be either discrete or continuous. The Fokker-Planck equations mentioned in the previous sections are examples of such Markovian master equations. $W_\rho(\sigma|\sigma')$ denotes the rate of the transition $\sigma \stackrel{\rho}{\longrightarrow} \sigma'$ for the elementary process $\rho = \pm1, \pm2, ..., \pm r$. A path or history of the system corresponds to the succession of states and elementary processes:

$$\omega_0\omega_1\omega_2\cdots = \sigma_0 \stackrel{\rho_1}{\longrightarrow} \sigma_1 \stackrel{\rho_2}{\longrightarrow} \sigma_2 \stackrel{\rho_3}{\longrightarrow} \cdots \tag{4·2}$$

If the system was in contact with a single reservoir it would relax to a global equilibrium state, in which case the detailed balance conditions

$$P_{\rm eq}(\sigma')\, W_\rho(\sigma'|\sigma) = P_{\rm eq}(\sigma)\, W_{-\rho}(\sigma|\sigma') \tag{4·3}$$

would be satisfied for all the possible forward and backward transitions $\pm\rho$. In this case, the product of the ratios of the forward and backward transition rates along a cycle $\vec{C}$ of successive states would be equal to unity:

$$\text{equilibrium conditions:} \qquad \prod_{\sigma_i \in \vec{C}} \frac{W_{\rho_i}(\sigma_{i-1}|\sigma_i)}{W_{-\rho_i}(\sigma_i|\sigma_{i-1})} = 1 \tag{4·4}$$

However, if the system is in contact with several reservoirs at different temperatures or chemical potentials, such products do not vanish and define the affinities or thermodynamic forces which drive the system out of equilibrium:[54)]

$$\text{nonequilibrium conditions:} \qquad \prod_{\sigma_i \in \vec{C}} \frac{W_{\rho_i}(\sigma_{i-1}|\sigma_i)}{W_{-\rho_i}(\sigma_i|\sigma_{i-1})} = \exp A(\vec{C}) \neq 1 \tag{4·5}$$

These affinities are given in terms of the external forces or torques acting on the nanosystem or the concentrations of the chemical species providing the energy to it. These considerations can be applied in particular to molecular motors.

4.2. *Biological nanomotors*

In biological systems, molecular motors are maintained in motion thanks to chemical energy coming from the hydrolysis of adenosine triphosphate:

$$\mathrm{ATP} \rightleftharpoons \mathrm{ADP} \ + \ \mathrm{P_i} \tag{4·6}$$

which is converted into its products, ADP and inorganic phosphate $\mathrm{P_i}$. At equilibrium in water, the concentrations are found in the ratio

$$\frac{[\mathrm{ATP}]_{\rm eq}}{[\mathrm{ADP}]_{\rm eq}\,[\mathrm{P_i}]_{\rm eq}} = \exp\frac{\Delta G^0}{k_{\rm B}T} \simeq 4.5\ 10^{-6}\ \mathrm{M}^{-1} \tag{4·7}$$

with the standard chemical Gibbs free energy difference $\Delta G^0 = -30.5$ kJ/mole $= -7.3$ kcal/mole $= -50$ pN nm. The system is out of equilibrium if the concentrations of the reactant and products are not in this precise ratio. We notice that the right-hand side is very small, which means that the concentration of ATP does not need to be very large to generate nonequilibrium conditions with available chemical free energy.

A famous nanomotor is the protein complex $\mathrm{F_1}$-ATPase which is able to drive the rotational motion of an actin filament or a bead glued to its shaft (see Fig. 3).[57),58)] Such a nanosystem may be found in different chemical states depending on whether ATP or its products is bonded to one of its catalytic sites. In each chemical state, the shaft of the motor is submitted to an internal torque deriving from some

free-energy potential $V_\sigma(\theta)$ which depends on the angle θ of the shaft. The motion of this angle is described by a Langevin-type equation

$$\zeta \frac{d\theta}{dt} = -\frac{\partial V_\sigma}{\partial \theta} + \tau_{\rm ext} + \tau_{\rm fluct}(t) \tag{4·8}$$

where ζ is the friction coefficient, $\tau_{\rm ext}$ is some external torque, and $\tau_{\rm fluct}(t)$ is the fluctuating torque due to the environment. This Langevin equation is the analogue of Eq. (2·7) for the case of overdamped rotational motion instead of underdamped translational motion. Moreover, the chemical state σ randomly jumps at each reactive event. These discrete random transitions are ruled by transition rates $W_{\rho,\sigma',\sigma}(\theta)$ which depend on the reaction, the chemical states, and the angle of the shaft. As soon as the chemical state changes, the shaft feels the new free-energy potential V_σ of the new chemical state. The mechanical motion of the shaft is thus coupled to the chemical reaction in these mechano-chemical processes. The master equation is here a set of coupled Fokker-Planck equations:

$$\partial_t\, p_\sigma(\theta,t) + \partial_\theta J_\sigma = \sum_{\rho,\sigma'} \left[p_{\sigma'}(\theta,t)\; W_{\rho,\sigma',\sigma}(\theta) - p_\sigma(\theta,t)\; W_{-\rho,\sigma,\sigma'}(\theta) \right] \tag{4·9}$$

where $p_\sigma(\theta,t)$ is the probability density to find the motor in the chemical state σ and the angle θ at time t and

$$J_\sigma = -D\;\partial_\theta p_\sigma + \frac{1}{\zeta}\left(-\partial_\theta V_\sigma + \tau_{\rm ext}\right) p_\sigma \tag{4·10}$$

with the diffusion coefficient $D = k_{\rm B}T/\zeta$.[59] The transition rates can be determined by Arrhenius' law in terms of transition-state free energy potentials.

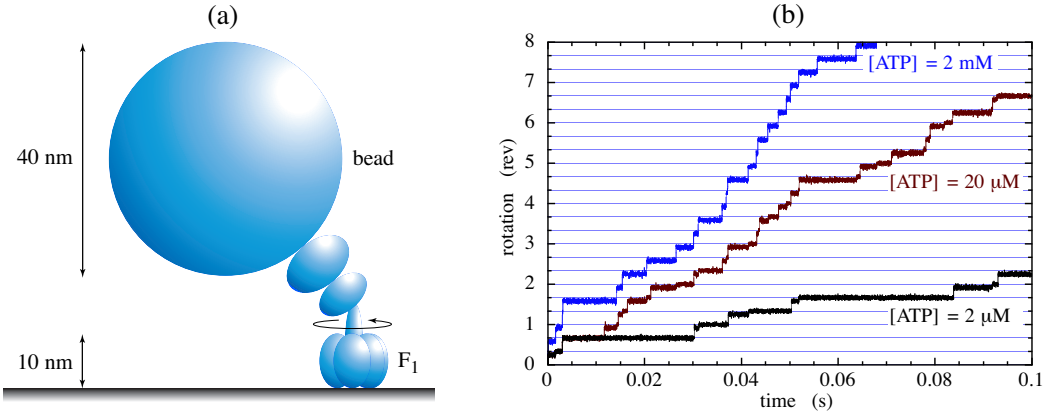

Fig. 3. (a) Schematic representation of the F_1-ATPase motor with a glued bead of diameter $d = 40$ nm.[58] (b) Stochastic trajectories showing the rotation of the shaft of the motor for different concentrations of ATP.[60]

The equations (4·9) admits an equilibrium state solution if the concentrations of the chemical species are in the equilibrium ratio (4·7), in which case the detailed balance conditions are satisfied. The mean rotation rate of the shaft vanishes at

equilibrium. If the concentrations are out of equilibrium, the motor is in a nonequilibrium steady state with a mean rotation rate which is now different from zero. The mean rotation rate is a highly nonlinear function of the chemical concentrations with a Michaelis-Menten dependence on the concentration of ATP.[60] Figure 3 depicts the nonequilibrium rotation of the shaft of the F_1-ATPase motor with a glued bead of diameter $d = 40$ nm simulated by a model with six chemical states and continuous angle.[60] We observe that the model nicely reproduces the jumps of the angle, as observed experimentally.[58]

The F_1-ATPase motor can also be modeled by the master equation (4·1) with discrete chemical states and corresponding discrete angular positions of the shaft. As shown below, a fluctuation theorem rules the stochastic rotation of the motor.

4.3. *Electric current in mesoscopic conductors and ion channels*

Nonequilibrium stochastic processes also take place in conductors of micrometric or nanometric sizes. Modern technology allows the observation of the number of charges inside the conductor. This number is a discrete random variable which obeys a master equation such as Eq. (4·1). The charges are injected in the conductor by a difference of potential at the contacts with the external circuit so that a mean current crosses the device. The affinity is here given by the difference of electric potential V as $A = eV/(k_{\rm B}T)$ where e is the electron charge. The fluctuation properties of the current can also be studied thanks to the master equation, leading to a full counting statistics.[19] An ion channel in a membrane can also be modeled by such master equations.[19] In spite of the fact that these systems are out of equilibrium they obey general relations known as fluctuation theorems.

§5. Fluctuation theorems and nonlinear response

5.1. *Fluctuation theorem for the currents*

As in first-passage problems, different properties can be studied along the paths or histories (4·2) of a nanosystem in a nonequilibrium steady state. This can be the number of electric charges crossing a conductor, the number of revolutions of a F_1 molecular motor, the number of ATP consumed or synthetized, or the work dissipated. If the system is in a nonequilibrium steady state, each one of these properties has a nonvanishing mean value. Nevertheless, these properties are affected by fluctuations because the size of nanosystems is close to the atomic scale. Therefore, it is possible to find fluctuations which are opposite to the mean value. Quite remarkably, the ratio of the probabilities of positive to negative fluctuations turns out to be simply related to the affinity or thermodynamic force responsible for the mean value as a consequence of the condition (4·5). If the properties of interest are the fluctuating currents $j_\gamma(t)$ crossing the system under the affinity or thermodynamic force A_γ, we have

$$\frac{P\left\{\frac{1}{t}\int_0^t j_\gamma(t')dt' \simeq +\alpha_\gamma\right\}}{P\left\{\frac{1}{t}\int_0^t j_\gamma(t')dt' \simeq -\alpha_\gamma\right\}} \simeq \exp\sum_\gamma A_\gamma\alpha_\gamma t \tag{5·1}$$

for $t \to \infty$. The integrals $\int_0^t j_\gamma(t')dt'$ are the number of electric charges or particles crossing the system during the time interval t. The proof of this fluctuation theorem for the currents is given elsewhere.[17)–19)]

5.2. *Fluctuation theorem for the dissipated work*

For an isothermal process, the work dissipated along a path can be defined as

$$\mathcal{W}_{\rm diss}(t) \equiv k_{\rm B}T \ \ln \frac{W_{\rho_1}(\sigma_0|\sigma_1)W_{\rho_2}(\sigma_1|\sigma_2)\cdots W_{\rho_m}(\sigma_{m-1}|\sigma_m)}{W_{-\rho_1}(\sigma_1|\sigma_0)W_{-\rho_2}(\sigma_2|\sigma_1)\cdots W_{-\rho_m}(\sigma_m|\sigma_{m-1})} \tag{5·2}$$

which obeys the following fluctuation theorem for $t \to \infty$:

$$\frac{P\left\{\frac{1}{t}\mathcal{W}_{\rm diss}(t) \simeq +p\right\}}{P\left\{\frac{1}{t}\mathcal{W}_{\rm diss}(t) \simeq -p\right\}} \simeq \exp\frac{p\,t}{k_{\rm B}T} \tag{5·3}$$

where p is a value for the dissipated power.[14),16)] In the nonequilibrium steady state, the entropy production is related to the mean values of the dissipated work and the currents by

$$\frac{d_{\rm i}S}{dt}\Big|_{\rm neq} = \frac{1}{T} \lim_{t\to\infty} \frac{\langle \mathcal{W}_{\rm diss}(t)\rangle}{t} = k_{\rm B}\sum_\gamma A_\gamma\, J_\gamma \geq 0 \tag{5·4}$$

where $J_\gamma = \langle j_\gamma \rangle$.

5.3. *Examples*

5.3.1. Drift under an external force

The fluctuation theorem for the current of a charged particle in an external force field can be formulated in terms of escape rates. The mean current of particles is given by the velocity v of the particles and their density n according to $J = nv$. The time integral of the fluctuating current of a single charge is thus the displacement of the charge:

$$\int_0^t j(t')\,dt' = \int_0^t v(t')\,dt' = x_t - x_0 \tag{5·5}$$

The biaised random walk of the particle can be described by the Fokker-Planck equation (3·7). The trajectories are random and we can look for the probability that the particle precisely travels with the velocity v during the time interval t. Most trajectories drift at the mean velocity $v = \mu F$. Therefore, the trajectories escape from the phase-space regions corresponding to the other values $v \neq \mu F$ of the drift velocity. The set of trajectories with some drift velocity $v \neq \mu F$ is of zero probability and we should expect that the trajectories escape out of this set with an escape rate $\Gamma(v)$ depending on the drift velocity:[4),6)]

$$P\left\{\frac{x_t - x_0}{t} \simeq v\right\} \sim \exp\left[-\Gamma(v)\,t\right] \tag{5·6}$$

For deterministic chaotic systems, this escape rate is given by Eq. (3·20) in terms of the Lyapunov exponents and the Kolmogorov-Sinai entropy per unit time. According

to the fluctuation theorem for the currents (5·1), the escape rates for positive and negative values of the drift velocity are related by

$$\Gamma(-v) - \Gamma(v) = \frac{Fv}{k_{\rm B}T} \tag{5·7}$$

The fluctuation theorem (5·3) for the dissipated work gives the same result since $p = Fv$ is the dissipated power. Similar relations have been obtained for other interesting systems such as nonequilibrium chemical reactions.[16),17)]

5.3.2. Biological nanomotors

The fluctuation theorem for the currents also applies to molecular motors such as the rotary F_1-ATPase.[20)] The current is here the reaction speed of ATP hydrolysis or the rotation speed of the shaft of the motor. Both are related to each other since three ATP molecules are required for a 360° revolution of the shaft. The motor can be modeled by a Markovian process with six discrete states corresponding to the experimentally observed substeps. In this context, it is possible to show that the probability distribution of the random number of revolutions R_t obeys

$$\frac{P\{R_t = r\}}{P\{R_t = -r\}} = \exp\frac{Ar}{k_{\rm B}} = \exp\left(3\frac{\Delta G - \Delta G^0}{k_{\rm B}T}r\right) \tag{5·8}$$

where A is the affinity of ATP hydrolysis, ΔG^0 is its standard Gibbs free energy as in Eq. (4·7), and $\Delta G = k_{\rm B}T\ln([{\rm ATP}]/[{\rm ADP}][{\rm P_i}])$.[20)] The factor three means that a full revolution consumes three ATP molecules, each one providing the free energy $\Delta G - \Delta G^0$. Accordingly, the statistical analysis of the fluctuating motion allows one to determine the thermodynamic affinity of the reaction.

5.4. *Linear and nonlinear response coefficients*

In nonequilibrium steady states, the mean currents crossing the system are functions of the affinities or thermodynamic forces:

$$J_\alpha = \sum_\beta L_{\alpha\beta}\,A_\beta + \frac{1}{2}\sum_{\beta,\gamma} M_{\alpha\beta\gamma}\,A_\beta\,A_\gamma + \frac{1}{6}\sum_{\beta,\gamma,\delta} N_{\alpha\beta\gamma\delta}\,A_\beta\,A_\gamma\,A_\delta + \cdots \tag{5·9}$$

The coefficients $L_{\alpha\beta}$ are Onsager's linear-response coefficients. The other coefficients characterize the nonlinear response of the system. The nonlinearity of the response is a main feature of chemical and biochemical systems. It has been shown that the molecular motors are also functioning very far from the linear regime.[20)]

A consequence of the fluctuation theorem for the currents (5·1) is that these coefficients obey remarkable relations,[17)–19)] the first of which are Onsager reciprocity relations:

$$L_{\alpha\beta} = L_{\beta\alpha} = \frac{1}{2}\int_{-\infty}^{+\infty} \langle[j_\alpha(t) - \langle j_\alpha\rangle]\,[j_\beta(0) - \langle j_\beta\rangle]\rangle_{\rm eq}\,dt = \lim_{t\to\infty}\frac{1}{2t}\langle \Delta G_\alpha(t)\Delta G_\beta(t)\rangle_{\rm eq} \tag{5·10}$$

with the Helfand moment $G_\alpha(t) = \int_0^t j_\alpha(t')dt'$ associated with the fluctuating current $j_\alpha(t)$ and $\Delta G_\alpha = G_\alpha - \langle G_\alpha\rangle$. Next, the third-order response coefficients can be

expressed as

$$M_{\alpha\beta\gamma} = \tilde{R}_{\alpha\beta,\gamma} + \tilde{R}_{\alpha\gamma,\beta} \tag{5·11}$$

in terms of the sensitivity of the linear-response coefficients to nonequilibrium perturbations:

$$\tilde{R}_{\alpha\beta,\gamma} \equiv \frac{\partial}{\partial A_\gamma} \lim_{t\to\infty} \frac{1}{2t} \langle \Delta G_\alpha(t) \Delta G_\beta(t) \rangle_{\rm neq} \Big|_{\{A_\epsilon=0\}} \tag{5·12}$$

Furthermore, the fourth-order response coefficients are given by

$$N_{\alpha\beta\gamma\delta} = \tilde{T}_{\alpha\beta,\gamma\delta} + \tilde{T}_{\alpha\gamma,\beta\delta} + \tilde{T}_{\alpha\delta,\beta\gamma} - \tilde{S}_{\alpha\beta\gamma,\delta} \tag{5·13}$$

in terms of

$$\tilde{T}_{\alpha\beta,\gamma\delta} = \frac{\partial}{\partial A_\gamma} \frac{\partial}{\partial A_\delta} \lim_{t\to\infty} \frac{1}{2t} \langle \Delta G_\alpha(t) \Delta G_\beta(t) \rangle_{\rm neq} \Big|_{\{A_\epsilon=0\}} \tag{5·14}$$

which are similar to the coefficients (5·12), and

$$\tilde{S}_{\alpha\beta\gamma,\delta} = \frac{\partial}{\partial A_\delta} \lim_{t\to\infty} \frac{1}{2t} \langle \Delta G_\alpha(t) \Delta G_\beta(t) \Delta G_\gamma(t) \rangle_{\rm neq} \Big|_{\{A_\epsilon=0\}} \tag{5·15}$$

which can be proved to be totally symmetric under all the permutations of the four indices.[18),19)] Such relations also hold at higher orders.

§6. Time asymmetry in dynamical randomness

It is intuitively well known that irreversible processes are not symmetric under time reversal. This observation is mathematically expressed by the positivity of entropy production in nonequilibrium systems, but the explanation is elusive for the lack of understanding based on the microscopic dynamics. As discussed in Sec. 2, it is important to point out that the microreversibility of the Hamiltonian dynamics does not preclude the time asymmetry of the actual trajectory followed by the system.[29)] This remark also concerns open systems in nonequilibrium steady states such as an electric resistance conducting a current. In this case, the charged particles enter the resistance with random positions and velocities but they exit the resistance with positions and velocities which are determined by the microscopic dynamics resulting from their interaction with the atoms of the resistance. The charged particles dissipate energy during their path inside the resistance. Reversing the process would require that the particles enter the resistance with exceptional positions and velocities allowing them to gain energy. This reasoning shows that, in nonequilibrium steady states, the paths of a system have a different probability weight than their time reversals:

$$\text{nonequilibrium steady state:} \qquad \mu(\omega_0\omega_1\omega_2\cdots\omega_{n-1}) \neq \mu(\omega_{n-1}\cdots\omega_2\omega_1\omega_0) \tag{6·1}$$

This means that the invariant probability measure describing a nonequilibrium steady state explicitly breaks the time-reversal symmetry.[5),6)] As explained in Sec. 2, there is no contradiction with the microreversibility of Liouville's equation because the invariant probability measure is a solution of Liouville's equation and a solution can have a lower symmetry than the equation itself.

It is quite remarkable that the ratio of the probability of a path to the probability of its reversal increases exponentially at a rate which is the entropy production of the steady state:

$$\frac{\mu(\omega_0\omega_1\omega_2\cdots\omega_{n-1})}{\mu(\omega_{n-1}\cdots\omega_2\omega_1\omega_0)} \sim \exp\left(\frac{d_{\rm i}S}{dt}\,t\right) \tag{6·2}$$

for almost all the typical paths in the limits $t = n\Delta t \to \infty$ and of a vanishing sampling time $\Delta t \to 0$.[24),25)] The entropy is here taken in the units of Boltzmann's constant $k_{\rm B}$. Moreover, if we take the average with respect to the probability distribution of the paths themselves, we obtain the entropy production as

$$\frac{d_{\rm i}S}{dt} = h^{\rm R} - h \tag{6·3}$$

in the limit $\Delta t \to 0$, where

$$h = \lim_{n\to\infty} -\frac{1}{n\Delta t} \sum_{\omega_0\omega_1\omega_2\cdots\omega_{n-1}} \mu(\omega_0\omega_1\omega_2\cdots\omega_{n-1})\,\ln\mu(\omega_0\omega_1\omega_2\cdots\omega_{n-1}) \tag{6·4}$$

is the entropy per unit time of Eq. (3·18) characterizing the dynamical randomness of the paths, while

$$h^{\rm R} = \lim_{n\to\infty} -\frac{1}{n\Delta t} \sum_{\omega_0\omega_1\omega_2\cdots\omega_{n-1}} \mu(\omega_0\omega_1\omega_2\cdots\omega_{n-1})\,\ln\mu(\omega_{n-1}\cdots\omega_2\omega_1\omega_0) \tag{6·5}$$

is the time-reversed entropy per unit time characterizing the dynamical randomness of the time reversals.[24),25)] We notice that the difference between these entropies per unit time is always non-negative in agreement with the second law of thermodynamics:

$$\frac{d_{\rm i}S}{dt} = \lim_{n\to\infty} \frac{1}{n\Delta t} \sum_{\omega_0\omega_1\omega_2\cdots\omega_{n-1}} \mu(\omega_0\omega_1\omega_2\cdots\omega_{n-1})\,\ln\frac{\mu(\omega_0\omega_1\omega_2\cdots\omega_{n-1})}{\mu(\omega_{n-1}\cdots\omega_2\omega_1\omega_0)} \geq 0 \tag{6·6}$$

The entropy production is thus given in terms of a path average involving the ratio of the forward to backward path probabilities. The consequences in biology are discussed here below.

§7. Conclusions

Recent advances in nanosciences have shown that collective properties which are traditionally studied in macroscopic systems already exist on all the spatial scales down to the nanometer just above the atomic scale. On all these scales, the collective properties are affected by the molecular fluctuations which become negligible for the macroscopic systems but are important in nanosystems. Therefore, the description of the properties of nanosystems requires the use of statistical mechanics. Nanosystems can be in nonequilibrium or equilibrium statistical states whether energy is dissipated on average or not. Here, we have described nanosystems which are out of equilibrium and some of their properties.

Such nanosystems can evolve by relaxation toward an equilibrium state as shown in Sec. 2. In this case, the relaxation is characterized by the decay rates which can be obtained as the Pollicott-Ruelle resonances of the Liouvillian dynamics, i.e., the dynamics of the statistical ensembles of trajectories. This method applies to the friction in sliding carbon nanotubes where the dynamic friction coefficient is given by Kirkwood formula of nonequilibrium statistical mechanics. The Pollicott-Ruelle resonances also rule the time evolution of first-passage problems in nanosystems. Several examples are given in Sec. 3 such as effusion, evaporation of hot nanoclusters, diffusion and mobility, as well as shear viscosity and heat conductivity as they can be considered in nanohydrodynamics. In these problems, the leading Pollicott-Ruelle resonance is an escape rate which can be related to the growth rate of volumes in the position space of the nanosystem and to the decay rate of the probabilities of the path or history of the nanosystem during some time interval before escape. The decay rate of the path probabilities characterizes the dynamical randomness of the paths and defines the so-called entropy per unit time.

The fluctuation properties of the paths or histories during some time interval also concern nanosystems maintained out of equilibrium such as biological nanomotors, mesoscopic conductors, and ion channels. Nanosystems in nonequilibrium steady states can be described in terms of stochastic processes as summarized in Sec. 4. The transitions rates of the stochastic process depend on the affinities or thermodynamic forces imposed by the external reservoirs of heat or particles and determining whether the nanosystem is maintained out of equilibrium or not. As a consequence of microreversibility, the fluctuations of the currents and the dissipated work obey fluctuation theorems as discussed in Sec. 5. From the fluctuation theorem for the currents, it is possible to deduce relations which generalize Onsager's reciprocity relations to the nonlinear response coefficients.

In Sec. 6, we have shown that the thermodynamic entropy production can be expressed in terms of the ratio of the path probabilities to the probabilities of their time reversals or, equivalently, by Eq. (6·3) as the difference between a newly introduced time-reversed entropy per unit time[24),25)] and the entropy per unit time previously introduced by Shannon, Kolmogorov, and Sinai.[26)–28)] These quantities characterize the dynamical randomness of the paths observed either forward or backward in time but averaged in both cases over the typical paths of the forward process. In nonequilibrium stead states, a time asymmetry appears between both quantities, which results into a positive difference equal to the thermodynamic entropy production. Thanks to the interpretation of the entropies per unit time as measures of the respective temporal disorder in the forward paths and their time reversals, Eq. (6·3) provides us with a most remarkable understanding of the second law of thermodynamics. Indeed, it proves that, in nonequilibrium steady states, the temporal disorder of the typical paths is lower than for the time-reversal paths. We here have a fundamental *principle of temporal ordering*, which is a corollary of the second law of thermodynamics. This temporal ordering is obtained at the price of an increase in time of the spatial disorder so that there is no contradiction with Boltzmann's interpretation of the second law. However, Eq. (6·3) changes the perspectives of the second law in emphasizing its constructive role in the *temporal aspects* of nonequi-

librium systems. In this regard, Eq. (6·3) expresses the intuitive property that the motion is more ordered out of equilibrium than at equilibrium. It is remarkable that this time asymmetry between the forward and backward dynamical randomnesses is directly related to the entropy production. The consequences of this new result are especially important for biology since it explains how the nonequilibrium can induce this temporal ordering which is so characteristic of biological phenomena. Moreover, it suggests that the genesis of biological information out of disorder is a natural consequence of driving out of equilibrium systems with the ability to store and retrieve molecular information.

Acknowledgements

This research is financially supported by the "Communauté française de Belgique" ("Actions de Recherche Concertées", contract No. 04/09-312).

References

1) P. Gaspard and G. Nicolis, Phys. Rev. Lett. **65** (1990) 1693.
2) P. Gaspard and F. Baras, Phys. Rev. E **51** (1995) 5332.
3) J. R. Dorfman and P. Gaspard, Phys. Rev. E **51** (1995) 28.
4) P. Gaspard and J. R. Dorfman, Phys. Rev. E **52** (1995) 3525.
5) S. Tasaki, and P. Gaspard, J. Stat. Phys. **81** (1995) 935.
6) P. Gaspard, *Chaos, Scattering and Statistical Mechanics* (Cambridge University Press, Cambridge UK, 1998).
7) P. Gaspard, I. Claus, T. Gilbert, and J. R. Dorfman, Phys. Rev. Lett. **86** (2001) 1506.
8) T. Gilbert, J. R. Dorfman, and P. Gaspard, Nonlinearity **14** (2001) 339.
9) D. J. Evans, E. G. D. Cohen, and G. P. Morriss, Phys. Rev. Lett. **71** (1993) 2401.
10) D. J. Evans and D. J. Searles, Phys. Rev. E **50** (1994) 1645.
11) G. Gallavotti and E. G. D. Cohen, Phys. Rev. Lett. **74** (1995) 2694.
12) J. Kurchan, J. Phys. A: Math. Gen. **31** (1998) 3719.
13) G. E. Crooks, Phys. Rev. E **60** (1999) 2721.
14) J. L. Lebowitz and H. Spohn, J. Stat. Phys. **95** (1999) 333.
15) C. Maes, J. Stat. Phys. **95** (1999) 367.
16) P. Gaspard, J. Chem. Phys. **120** (2004) 8898.
17) D. Andrieux and P. Gaspard, J. Chem. Phys. **121** (2004) 6167.
18) D. Andrieux and P. Gaspard, preprint cont-mat/0512254 (2005).
19) D. Andrieux and P. Gaspard, J. Stat. Mech.: Th. Exp. (2006) P01011.
20) D. Andrieux and P. Gaspard, *Fluctuation theorems and the nonequilibrium thermodynamics of molecular motors*, preprint (2006).
21) C. Jarzynski, Phys. Rev. Lett. **78** (1997) 2690.
22) C. Bustamante, J. Liphardt, and F. Ritort, Phys. Today **58** (2005) 43.
23) D. Collin, F. Ritort, C. Jarzynski, S. B. Smith, I. Tinoco Jr., and C. Bustamante, Nature **437** (2005) 231.
24) P. Gaspard, J. Stat. Phys. **117** (2004) 599.
25) P. Gaspard, New. J. Phys. **7** (2005) 77.
26) C. Shannon, Bell System Tech. J. **27** (1948) 379, 623.
27) A. N. Kolmogorov, Dokl. Akad. Nauk SSSR **124** (1959) 754.
28) Ya. G. Sinai, Dokl. Akad. Nauk SSSR **124** (1959) 768.
29) P. Gaspard, in: P. Collet et al. (Editors), *Chaotic Dynamics and Transport in Classical and Quantum Systems* (Kluwer Academic Publishers, Dordrechts, 2005).
30) I. P. Cornfeld, S. V. Fomin, and Ya. G. Sinai, *Ergodic Theory* (Springer-Verlag, Berlin, 1982).
31) M. Pollicott, Invent. Math. **81** (1985) 413; Invent. Math. **85** (1986) 147.
32) D. Ruelle, Phys. Rev. Lett. **56** (1986) 405; J. Stat. Phys. **44** (1986) 281.

33) P. Gaspard and D. Alonso Ramirez, Phys. Rev. A **45** (1992) 8383.
34) R. Blümel and U. Smilansky, Phys. Rev. Lett. **60** (1988) 477.
35) W. Lu, M. Rose, K. Pance, and S. Sridhar, Phys. Rev. Lett. **82** (1999) 5233.
36) W. Lu, L. Viola, K. Pance, M. Rose, and S. Sridhar, Phys. Rev. E **61** (2000) 3652.
37) K. Pance, W. Lu, and S. Sridhar, Phys. Rev. Lett. **85** (2000) 2737.
38) T. Prosen, Physica D **187** (2004) 244.
39) M. Esposito and P. Gaspard, Phys. Rev. B **71** (2005) 214302.
40) M. Esposito and P. Gaspard, J. Stat. Phys. **121** (2005) 463.
41) J. Servantie and P. Gaspard, Phys. Rev. Lett. **91** (2003) 185503.
42) J. Servantie and P. Gaspard, Phys. Rev. B (2006).
43) J. G. Kirkwood, J. Chem. Phys. **14** (1946) 180.
44) A. M. Fennimore, T. D. Yuzvinsky, W.-Q. Han, M. S. Fuhrer, J. Cumings, and A. Zettl, Nature **424** (2003) 408.
45) R. K. Pathria, *Statistical Mechanics* (Pergamon Press, Oxford, 1972).
46) F. Chandezon, S. Bjørnholm, J. Borggreen, and K. Hansen, Phys. Rev. B **55** (1997) 5485.
47) T. Tél, J. Vollmer, and W. Breymann, Europhys. Lett. **35** (1996) 659.
48) E. Helfand, Phys. Rev. **119** (1960) 1.
49) M. S. Green, J. Chem. Phys. **20** (1952) 1281; **22** (1954) 398.
50) R. Kubo, J. Phys. Soc. Jpn. **12** (1957) 570.
51) S. Viscardy and P. Gaspard, Phys. Rev. E **68** (2003) 041204.
52) S. Viscardy and P. Gaspard, Phys. Rev. E **68** (2003) 041205.
53) G. Nicolis, J. Stat. Phys. **6** (1972) 195.
54) J. Schnakenberg, Rev. Mod. Phys. **48** (1976) 571.
55) G. Nicolis and I. Prigogine, *Self-Organization in Nonequilibrium Systems* (Wiley, New York, 1977).
56) Luo Jiu-li, C. Van den Broeck, and G. Nicolis, Z. Phys. B - Cond. Matt. **56** (1984) 165.
57) H. Noji, R. Yasuda, M. Yoshida, and K. Kinosita Jr., Nature **386** (1997) 299.
58) R. Yasuda, H. Noji, M. Yoshida, K. Kinosita Jr., and H. Itoh, Nature **410** (2001) 898.
59) F. Jülicher, A. Ajdari, and J. Prost, Rev. Mod. Phys. **69** (1997) 1269.
60) E. Gerritsma and P. Gaspard, *Mechanochemical model for F_1-ATPase molecular motor*, preprint (2006).